

scribed by Cohn.¹ Figure 1(a) shows the cross-sectional view of Cohn's device; the printed-circuit (strip transmission line) equivalent is shown in Fig. 1(b). The design of the coaxial version is determined by characteristic impedances Z_{01} (the impedance of a bar of width w and height b_2 placed within a ground plane spacing b_1) and Z_{02} (the impedance of the inner coaxial lines).

The printed-circuit version of the coupler is fabricated from commercially available copper-clad dielectric material and is designed to produce the same Z_{01} and Z_{02} values that are used in Fig. 1(a). The Z_{01} impedance is determined from the impedance of a metallic bar of width w_2 and height b_2 placed within a ground plane spacing b_1 . The Z_{02} value is obtained from the impedance of a strip of thickness t and width w_1 placed within a ground plane spacing b_2 . The two inner strips are assumed to be decoupled; $s/b_2 > 0.5$ satisfies this condition for a 3-dB coupler.

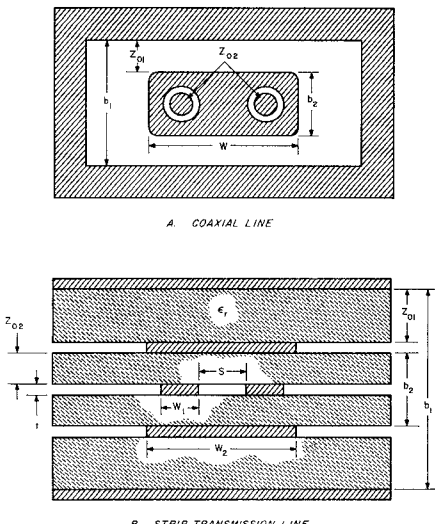


Fig. 1. Re-entrant cross sections.

A single-section 3-dB coupler using this technique was designed for the 450- to 850-Mc/s range. The experimental results are shown in Fig. 2. The coupling from ports 1 to 3 vs. frequency agrees with the theory within 0.15 dB; the SWR and isolation (insertion loss from ports 1 to 4) are comparable to values obtained with coaxial designs. The insertion loss between ports 1 and 2 is 0.25 dB higher than the theoretical; this is attributed to dissipation. These data were obtained with no experimental adjustments of the calculated parameters. This tends to demonstrate that no dimensionally critical spacings are required within the structure. This technique has been used successfully at frequencies as high as 4 Gc/s.

In summary, printed-circuit equivalents of Cohn's re-entrant coupler have been successfully designed and constructed. The tolerances inherent in the etching process are not serious in designs up to at least 4 Gc/s. The printed circuit version should, therefore, be inexpensive to produce and practical.

¹ S. B. Cohn, "Re-entrant cross section and wide-band 3-dB hybrid coupler," *IEEE Trans. on Microwave Theory and Techniques*, vol. MTT-11, pp. 254-258, July 1963.

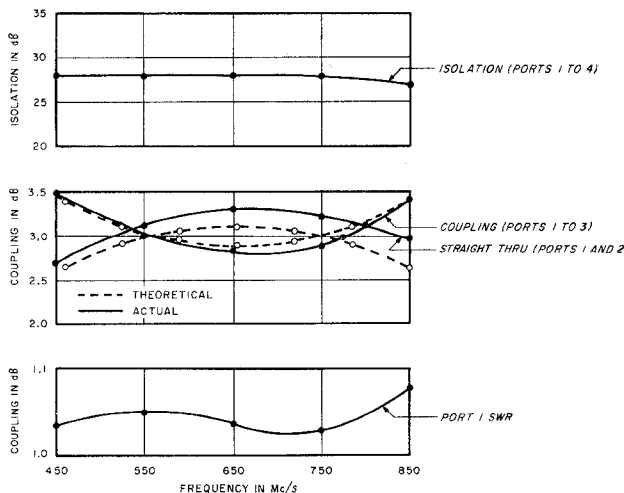


Fig. 2. Strip transmission line 3-dB re-entrant coupler.

to design to performance specifications comparable to that obtained with coaxial re-entrant couplers.

L. LAVENDOL
J. J. TAUB
Airborne Instruments Lab.
Cutler-Hammer, Inc.
Deer Park, N. Y.

for stable operation. The filter assembly, which was pressurized with 50 psig of air, experienced breakdown at 4.5-MW peak and 8.1-kW average. The threshold of breakdown for this unit was inaudible and could only be detected when seen through a viewing bend. When disassembled, burn marks were noted at the four corners of teeth in three center rows of waffle-iron I.

At this point in the program, consideration was given to a waffle-iron filter which utilized round teeth. This round tooth unit was a later version of the square tooth model [3] and was purported to improve the high power capability by a factor of 1.3. One such round tooth model of waffle I was fabricated and tested to a breakdown level of 4-MW peak and 7.1-kW average at 45 psig. This approach was dropped after assurances that breakdown was not due to extraneous causes.

To increase the high power capability of the square tooth filter, certain modifications were required. These modifications included: 1) an increase in tooth spacing and 2) a severe rounding of the teeth in the three center rows of waffle-iron I. The increase in tooth spacing of waffle-iron I resulted in a narrower stop band since the cutoff frequency of the filter was increased. The change of tooth surface area in waffle-iron I resulted in a capacitance reduction and a subsequent VSWR increase at the lower end of the pass band. No modifications were made to waffle-iron sections II and III.

Both of these modifications to waffle-iron I were made in incremental steps and each step was marked by an improvement in the high power handling capability of the filter assembly. This is shown in Fig. 2. It can be seen that a level of 6.7-MW peak and 12 kW of average power was achieved at 50 psig. This capability sufficed for the particular application; therefore, no effort was made to increase the power handling characteristics beyond this level. From Fig. 2 it can also be seen that waffle-iron section I limited the high power capability of the assembly. waffle-iron filters sections II and III were capable of higher power levels of 50 psig.

Figure 3 indicates the VSWR in the pass band for various conditions. Final VSWR data for the assembly, which included two

Manuscript received June 7, 1965.

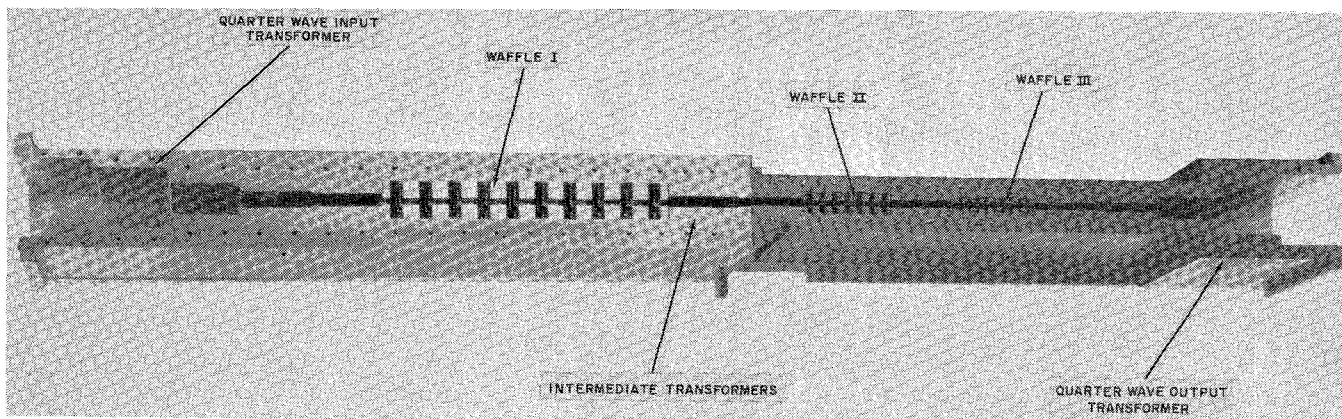


Fig. 1. L-band waffle-iron filter assembly.

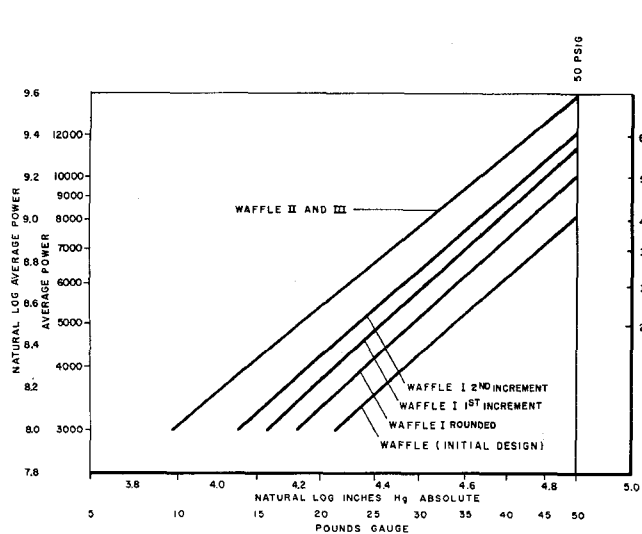


Fig. 2. Breakdown vs. pressure.

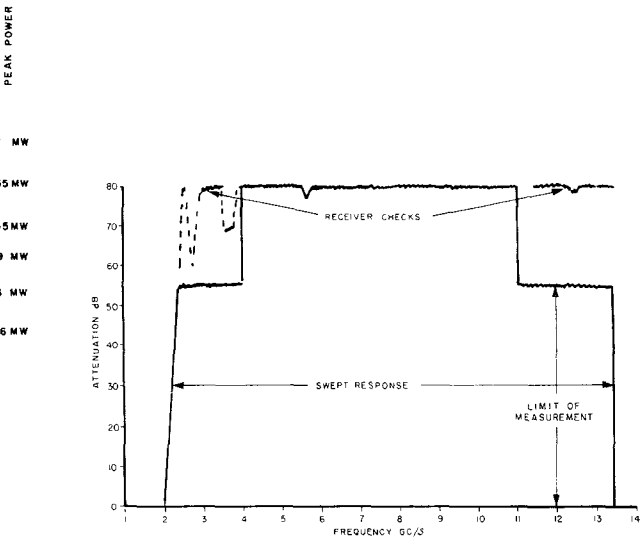


Fig. 4. Stop band attenuation.

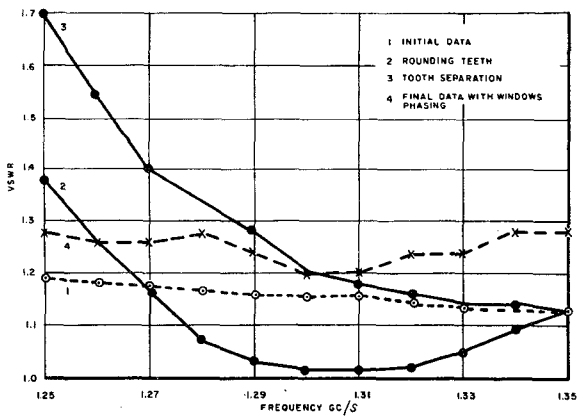


Fig. 3. VSWR vs. frequency.

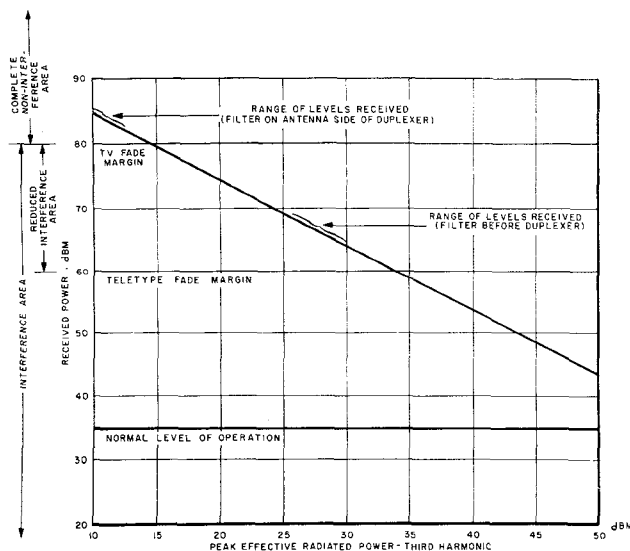


Fig. 5. Received power vs. radiated power at microwave station.

pressure windows, was 1.28 over the band of interest.

The measured stop band insertion loss is shown in Fig. 4. The insertion loss of the TE_{10} mode was measured using smooth tapered sections from waveguide connected directly to the input and output of the filter. A continuously swept signal generator was connected at the input and the filter output was monitored on a scope. A TWT amplifier operating from 4-11 Gs/c provided additional sensitivity throughout this band. The limit of measurements for the other frequencies of interest was 55 dB. Point-to-point receiver measurements were taken throughout the band of limited sensitivity.

A point of further interest concerned the location of the waffle-iron filter assembly relative to the radar system duplexer. Figure 5 illustrates the results of dynamic cooperative tests performed by the radar and a microwave link station operating at the subject radar's third harmonic frequency. The objectives of the test was to ascertain: 1) the effectiveness of this waffle-iron filter in reducing interference levels beyond the television fade margin of the microwave link and 2) to determine the optimum location for the waffle-iron filter assembly relative to the duplexer in the radar system.

It can be seen from the graph that the range of levels received with the waffle-iron filter before the duplexer were 5 dB below the fade margin for teletype but still within the television fade margin. Placing the filter on the antenna side of the duplexer resulted in mean signal levels 17 dBm below the previous reading. This data furnishes conclusive proof of TR tube harmonic radiation and the necessity for packaging such waffle-iron filters on the antenna side of the duplexers.

This correspondence has shown that waffle-iron filters can be utilized at moderate power levels at L -band. Higher levels could also be achieved by utilizing a technique of paralleling filters [3] using binary symmetrical power dividers. Thus, a double layer filter could be packaged within the dimensions of L -band waveguide. By dividing the power among two filters and then recombining their outputs, the power handling capacity is doubled.

Heavy wall construction was utilized (Fig. 1) to provide distortion free operation with high internal pressures. A considerable weight savings can be achieved if a ribbed construction were used with a thin wall thickness.

J. CAPUTO
F. BELL

Radiation Div.
Sperry Gyroscope Co.
Division of Sperry Rand Corp.
Great Neck, N. Y.

REFERENCES

- [1] G. L. Matthaei, L. Young, and E. M. T. Jones, "Design of microwave filters, impedance matching networks, and coupling structures," Standard Research Inst., Menlo Park, Calif., Proj. 3527, Contract DA 36-039 SC87398, January 1963.
- [2] E. Sharp, "A high-power wide-band waffle-iron filter," *IEEE Trans. on Microwave Theory and Techniques*, vol. MTT-11, pp. 111-116, March 1963.
- [3] Young and B. M. Schiffman, "New and improved types of waffle-iron filters," *Proc. IEE (London)*, vol. 110, July 1963.

Correction to "Exact Design of Band-Stop Microwave Filters"

In the above paper¹ the authors have called the following to the attention of the Editor:

The formula for Z_4 , for case $n=5$ in Table II (page 8), should have read

$$Z_4 = \frac{Z_A}{g_0} \left(\frac{1}{1 + \Lambda g_5 g_6} + \frac{g_6}{\Lambda g_4 (1 + \Lambda g_5 g_6)^2} \right).$$

B. M. SCHIFFMAN
Electromagnetic Techniques Lab.
Stanford Research Inst.
Menlo Park, Calif.

Manuscript received April 9, 1965.

¹ B. M. Schiffman and G. L. Matthaei, *IEEE Trans. on Microwave Theory and Techniques*, vol. MTT-12, pp. 6-15, January 1964.

The Electric Field and Wave Impedance in Spin Wave Propagation

The propagation of electromagnetic waves in magnetic materials, allowing exchange coupling, has been treated by Auld [1] and by Soohoo [2]. Their calculations involved the simultaneous solution of Maxwell's equations and the equation of motion of the magnetization, for plane waves.

According to the well known results of Auld [1] for ferrimagnetic materials, the susceptibility tensor is of the same form as the well-known Polder tensor for the uni-

Manuscript received March 22, 1965.

form mode, except that the internal static magnetic fields are augmented by an exchange field in the case of magnetic waves with a finite wave vector \mathbf{k} . Depending on the magnitude of \mathbf{k} , the various plane waves could be classified into electromagnetic, magnetostatic, and exchange types.

In the interpretation of these results, the statement has been made that as the spin wavelength becomes shorter and shorter, the RF electric field becomes increasingly smaller compared with the RF magnetic field and can eventually be neglected.

We suggest that this statement is perhaps somewhat too strong, for it is desirable to examine not only the ratios of absolute quantities of electric and magnetic fields, but such quantities as the transverse wave impedance. Here we find the general rule that as the wavelength decreases, the wave impedance increases. This is seen by substitution of a magnetic field intensity of form $[\hat{x}h_0 + \hat{y}h_1][\exp\{j(\omega t - kz)\}]$ into the Maxwell curl equation, in the absence of conduction current. The result is

$$e = [\hat{x}(h_1)(k/\omega_r \epsilon_0) + \hat{y}(-h_0)(k/\omega_r \epsilon_0)] \cdot \exp[j(\omega t - kz)] \quad (1)$$

so that

$$Z_{\text{transverse}} = |e_x/h_y| = |e_y/h_x| = k/\omega_r \epsilon_0. \quad (2)$$

As the wavelength gets shorter, k becomes larger; so that the ratio $|e/h|$ increases. At 10 Gc, for example, for $\epsilon_r = 15$, and for wavelength $\lambda_g = (5)(10^{-7})$ meters, $|e/h| = (1.5)(10^6)$ ohms. Direct substitution of the appropriate quantities into Auld's expressions yields essentially the same result.¹

¹ In private communications, Dr. Auld stated that he was aware of this and of the field structure. We appreciate Dr. Auld's kindness in communicating with us on this subject.

TABLE I
WAVE COMPONENTS FOR SPIN WAVE PROPAGATION, FOR CIRCULARLY POLARIZED RF MAGNETIZATION

The dc magnetic field is taken in the z direction. Propagation is in the $Y-Z$ Plane. Note that although the RF magnetization is circularly polarized, \mathbf{e} , \mathbf{h} , and \mathbf{b} are circularly polarized only for $\theta = 0^\circ$. For this table, the units are MKS rationalized, with $\mathbf{b} = \mu_0(\mathbf{h} - \mathbf{m})$; $\mathbf{e} = \epsilon_r \mathbf{e}_0$; $k_f = \omega(\epsilon \mu_0)^{1/2}$.

	$\theta_k = 0^\circ$	$\theta_k = 90^\circ$
\mathbf{m}	$m_0 \begin{bmatrix} -1 \\ j \\ 0 \end{bmatrix} e^{j[\omega t - kz]}$	$m_0 \begin{bmatrix} -1 \\ j \\ 0 \end{bmatrix} e^{j[\omega t - ky]}$
\mathbf{e}	$-m_0 \left(\frac{k_f}{k} \right) \left(\frac{\mu_0}{\epsilon} \right)^{1/2} \begin{bmatrix} -j \\ 1 \\ 0 \end{bmatrix} e^{j[\omega t - kz]}$	$m_0 \left(\frac{k_f}{k} \right) \left(\frac{\mu_0}{\epsilon} \right)^{1/2} \begin{bmatrix} 0 \\ 0 \\ -1 \end{bmatrix} e^{j[\omega t - ky]}$
\mathbf{h}	$m_0 \left(\frac{k_f}{k} \right)^2 \begin{bmatrix} 1 \\ j \\ 0 \end{bmatrix} e^{j[\omega t - kz]}$	$m_0 \begin{bmatrix} -(k_f/k)^2 \\ -j \\ 0 \end{bmatrix} e^{j[\omega t - ky]}$
\mathbf{b}	$\simeq \mu_0 m_0 \begin{bmatrix} -1 \\ j \\ 0 \end{bmatrix} e^{j[\omega t - kz]}$	$\mu_0 m_0 \begin{bmatrix} -1 \\ 0 \\ 0 \end{bmatrix} e^{j[\omega t - ky]}$